PLD2 fuels 5-fluorouracil resistance in colorectal cancer: Hypoxic hijacking of autophagy unveils a novel therapeutic vulnerability

KUNLI DU[1*], PENGFEI WANG[1*], XISHENG YANG[1*], YANJUN LU[2], YI WANG[2], WENDA WANG[2], JIANYONG ZHENG[1] and MAOXI LIU[2]

[1]Department of Digestive Surgery, Xijing Hospital of Digestive Diseases, Air Force Medical University, Xi'an, Shaanxi 710032, P.R. China; [2]Department of Colorectal Surgery, Shanxi Province Cancer Hospital, Shanxi Hospital Affiliated to Cancer Hospital, Chinese Academy of Medical Sciences, Cancer Hospital Affiliated to Shanxi Medical University, Taiyuan, Shanxi 030013, P.R. China

Received October 3, 2025; Accepted July 10, 2026

DOI: 10.3892/ijo.2026.5953

Abstract. The present study investigated the relationship between phospholipase D2 (PLD2) and hypoxia-induced chemoresistance in colorectal cancer (CRC) and elucidated its regulatory mechanisms. The present study demonstrated that increased PLD2 was associated with poor prognosis and chemoresistance in CRC via The University of Alabama at Birmingham cancer data analysis portal and Kaplan-Meier plotter databases and 5-fluorouracil (5-Fu)-resistant CRC tissues. The protein expression of PLD2, hypoxia-inducible factor 1 alpha (HIF-1α), multidrug resistance-associated protein 2 (MRP2), LC3-II/I, and Beclin-1 was markedly upregulated under hypoxia in SW620 and SW480 cells in a time-dependent manner. Next, SW620 and SW480 cells were transduced with recombinant replication-deficient adenoviral vectors encoding PLD2-targeting short hairpin (sh)RNA (Ad-sh-PLD2) or PLD2 overexpression (oe) constructs (Ad-oe-PLD2), followed by treatment with 5-Fu, rapamycin (Rapa), or 3-methyladenine (3-MA), either alone or in combination. *In vitro* data revealed that PLD2 promoted hypoxia-driven 5-Fu resistance by enhancing autophagy. Decreasing PLD2 expression increased tumor sensitivity to 5-Fu in a mouse xenograft model, an effect that was reversed by Rapa treatment. In conclusion, the findings suggested that PLD2 is associated with hypoxia-induced CRC chemoresistance by modulating autophagy, suggesting that PLD2 is a potential new therapeutic target.

Correspondence to: Dr Maoxi Liu, Department of Colorectal Surgery, Shanxi Province Cancer Hospital, Shanxi Hospital Affiliated to Cancer Hospital, Chinese Academy of Medical Sciences, Cancer Hospital Affiliated to Shanxi Medical University, 3 Zhigong Xinjie Street, Xinghualing, Taiyuan, Shanxi 030013, P.R. China
E-mail: liumaoxi1983@163.com

Dr Jianyong Zheng, Department of Digestive Surgery, Xijing Hospital of Digestive Diseases, Air Force Medical University, 169 Changle West Road, Xi'an, Shaanxi 710032, P.R. China
E-mail: zhjy68@163.com

*Contributed equally

Key words: phospholipase D2, colorectal cancer, hypoxia, autophagy, chemosensitivity

Introduction

Colorectal cancer (CRC) is the second most prevalent malignancy globally and ranks third in terms of tumor-related fatalities (1). Surgical intervention forms the foundation of treatment for patients with early-stage CRC, whereas chemotherapy is a commonly used measure to improve the prognosis of advanced or metastatic CRC (2). The predominant chemical agent for treating CRC is 5-fluorouracil (5-Fu) (3), which inhibits tumor growth by impeding thymidylate synthetase-mediated pyrimidine synthesis. Despite advances in chemotherapeutic regimens, the efficacy of 5-Fu is limited in most treated patients because of acquired resistance to drugs (4). Hence, elucidating the molecular mechanisms underlying 5-Fu resistance in CRC may offer new perspectives for overcoming chemotherapy resistance and enhancing therapeutic outcomes.

Hypoxia, a ubiquitous trait of solid tumors, endows tumor cells with the ability to adapt to nutritionally deprived and adverse microenvironments, thereby facilitating the preservation of their viability (5). Hypoxia within the tumor microenvironment markedly contributes to the development of resistance to chemotherapy in types of cancer, including CRC (6). This phenomenon is closely associated with the activation of autophagy (7). Autophagy is a key homeostatic process in the human body that accounts for the degradation and recycling of damaged or excessive proteins, lipids and organelles (8). Hypoxia-induced autophagy promotes tumor growth and aggressive behavior by providing nutrients and energy for the metabolism of cancer cells (9). For example, Yang *et al* (10) reported that hypoxia-induced cytoprotective autophagy counteracted gemcitabine-induced apoptosis by increasing HIF-1α

expression in bladder cancer. Notte *et al* (11) also reported that hypoxia triggers cytoprotective autophagy and consequently reduces the sensitivity of triple-negative breast cancer cells to Taxol treatment, suggesting that increasing oxygen tension might be a way to increase sensitivity to chemotherapy. Additionally, autophagy is upregulated in 5-Fu-resistant CRC cells, and an autophagy activator can increase the resistance of cells to 5-Fu (12,13). However, the molecular mechanisms by which autophagy regulates hypoxia-mediated resistance to chemotherapy in CRC remain unclear.

A member of the phospholipase D (PLD) family, PLD2 is a lipid-signaling enzyme that generates phosphatidic acid by catalyzing the hydrolysis of phosphatidylcholine (14). PLD2 has attracted considerable attention due to its critical regulatory roles in multiple signaling pathways involved in tumor progression. In metastatic breast cancer, PLD2 facilitates local invasion by regulating the plasma membrane targeting of Membrane-Type 1 Matrix Metalloproteinase (MT1-MMP) (15), while PLD2 inhibition reduces cell viability, colony formation, and directional movement in prostate cancer (16). In CRC, PLD2 is frequently overexpressed (17,18). Hypoxia, a common feature of solid tumors, contributes to chemoresistance by altering the expression and activity of genes and signaling pathways that support tumor cell survival. Our previous work demonstrated that hypoxia upregulates PLD2 expression and activity in CRC cells (19). Notably, inhibition of PLD2 under hypoxic conditions increases CRC cell apoptosis by inactivating the PI3K/AKT signaling pathway (20) and suppresses cell proliferation via downregulation of Cyclin D1 through NF-κBp65 signaling (21). PLD2 has also been implicated in hypoxia-induced therapy resistance in ovarian tumors (22). Autophagy is another mechanism contributing to cell survival under stress and can be monitored by the accumulation of LC3-II. PLD2 has been shown to regulate autophagy in CRC cells (23), suggesting that it may play a role in the hypoxia-induced adaptive responses of CRC. Based on these findings, we hypothesize that PLD2 participates in the regulation of autophagy and chemoresistance under hypoxic conditions in CRC.

Materials and methods

Bioinformatics analysis. The University of Alabama at Birmingham cancer data analysis portal (UALCAN; https://ualcan.path.uab.edu) (24) was used to examine the expression levels of PLD2 in The Cancer Genome Atlas datasets. To investigate the prognostic value of PLD2 expression in CRC, the Kaplan-Meier plotter (http://kmplot.com/analysis/) (25) was used. First, the tumor type 'CRC' was designated. The gene 'PLD2' was subsequently entered. Overall survival (OS) and recurrence-free survival (RFS) were both subsequently selected for analysis.

Tissue specimens. After the Ethics Committee of Shanxi Province Cancer Hospital (Shanxi, China; approval no. SPCH-87A; Date: 2021-1-21) approved the present study, the clinical CRC specimens were collected and included 5-Fu-resistant patients (n=20) and 5-Fu-sensitive patients (n=20) who underwent chemotherapy at this hospital between January 2021 and January 2023 (Table I). The selection criteria for patients were as follows: First, the diagnosis of CRC was confirmed through postoperative pathological examination. Second, the patients had received only 5-Fu-based chemotherapy before specimen collection. Third, written informed consent was obtained from each patient before the study commenced. Patients with prior neoadjuvant or other anticancer therapies, other malignancies, severe systemic diseases, incomplete clinical data, or insufficient tissue samples were excluded. Cases were deemed 5-Fu resistant if disease progression occurred during postoperative chemotherapy or if recurrence occurred within six months after initial chemotherapy. By contrast, 5-Fu-sensitive cases were identified by either recurrence occurring more than six months after primary chemotherapy or the absence of any recurrence.

RNA extraction and reverse transcription-quantitative (RT-q) PCR. Total RNA was extracted from the tissue samples with TRIzol® reagent (Invitrogen; Thermo Fisher Scientific, Inc.) according to the manufacturer's instructions. A SuperScript™ II Reverse Transcriptase Kit (Invitrogen; Thermo Fisher Scientific, Inc.) was used for RNA transcription to cDNA following the manufacturer's protocol. Quantitative real-time PCR was conducted on a CFX96 Real-Time System (Bio-Rad Laboratories, Inc.) using SYBR Premix Ex Taq™ (Takara Biotechnology Co., Ltd.) according to the manufacturer's instructions. The amplification process was as follows: Initial denaturation at 95˚C for 10 min, followed by 45 cycles of 10 sec at 95˚C, 30 sec at 60˚C and 20 sec at 85˚C. The sequences of primers used were: PLD2 forward, 5'-ATCGAGGACACA GAGACGGA-3', and reverse, 5'-ATCACAGATGGGGTC TCGGA-3'; GAPDH forward, 5'-GAAAGCCTGCCGGTG ACTAA-3', and reverse, 5'-TGGAATTTGCCATGGGTG GA-3'. The $2^{-\Delta\Delta Cq}$ method (26) was used to analyze the mRNA expression levels of PLD2.

Cell culture and treatments. The present study obtained two CRC cell lines, SW620 and SW480, from the Cell Bank of the Chinese Academy of Sciences, which routinely authenticates cell lines. The cells were cultured in RPMI-1640 medium supplemented with 10% heat-inactivated FBS, 50 U/ml streptomycin, and 50 U/ml penicillin (Gibco; Thermo Fisher Scientific, Inc.) at 37˚C in a humidified atmosphere containing 5% CO_2. Hypoxia treatment was performed by placing cells in a sealed chamber (Thermo Forma; Thermo Fisher Scientific, Inc.) with 1% O_2, 5% CO_2, and 94% N_2. For time-course experiments, cells were exposed to hypoxia for 0, 12, 24, or 48 h. In all functional experiments unless otherwise specified, cells were subjected to 24 h hypoxia following 48 h post-transduction stabilization. 5-Fu was applied at indicated concentrations for 24 h in all *in vitro* functional assays. Rapamycin (Rapa, 10 μM) (27) or 3-methyladenine (3-MA, 10 mM) (28) (MilliporeSigma) was administered 1-2 h prior to 5-Fu treatment and maintained throughout the treatment period.

Cell transduction. Recombinant replication-deficient adenoviral vectors encoding PLD2-targeting short hairpin RNA (Ad-sh-PLD2), PLD2 overexpression constructs (Ad-oe-PLD2), and their corresponding negative control adenoviruses (Ad-sh-NC and Ad-Vector) were purchased

Table I. Clinical characteristics of colorectal cancer patients with 5-Fu-sensitive and 5-Fu-resistant tissues.

Characteristics	5-Fu-sensitive (n=20)	5-Fu-resistant (n=20)
Age (mean ± SD)	61.2±10.5	63.4±9.8
Sex		
Male	12	11
Female	8	9
Tumor location		
Colon	13	11
Rectum	7	9
AJCC stage		
I-II	8	6
III-IV	12	14
Histological grade		
Low/Moderate	15	14
High	5	6

AJCC, American Joint Committee on Cancer; 5-Fu, 5-fluorouracil.

from Shanghai GenePharma Co., Ltd. SW620 and SW480 cells ($5x10^4$ cells per well) were seeded in six-well plates and cultured for 18 h prior to transduction. Cells were transduced with the recombinant adenoviruses at a multiplicity of infection (MOI) of 10 for 4 h at 37˚C in a humidified incubator containing 5% CO_2. MOI was determined based on preliminary optimization experiments and manufacturer guidance. Following transduction, the viral medium was removed and replaced with fresh complete culture medium. Cells were then cultured for an additional 48 h to allow efficient PLD2 knockdown or overexpression before subsequent experiments. The transduction efficiency was verified by western blot analysis of PLD2 expression.

Cell viability assay. Cell viability was assessed by conducting the Cell Counting Kit-8 (CCK-8) assay (Dojindo Laboratories, Inc.) following the manufacturer's instructions. Cells were seeded at $2.5x10^4$ cells per well in 96-well plates and cultured for 24 h. After the indicated treatments, 10 μl of CCK-8 reagent was added to each well and incubated for 2 h at 37˚C. Absorbance at 450 nm was measured using a microplate reader (Bio-Rad Laboratories, Inc.). The relative cell survival rate was calculated using the formula: cell survival rate (%)=(OD experimental-OD blank)/(OD control-OD blank) x100%. The half-maximal inhibitory concentration (IC_{50}) of 5-Fu was determined from the relative survival curve using GraphPad Prism v.8.0 (Dotmatics).

Colony formation assay. First, CRC cells from different groups (500 cells per well) were inoculated in six-well plates and cultured in RPMI-1640 medium supplemented with 10% FBS. After two weeks, the naturally formed colonies (>50 cells per colony) were fixed with 4% paraformaldehyde (MilliporeSigma) at room temperature for 20 min, stained with 0.5% crystal violet, and then observed under a light microscope (DM3000; Leica Microsystems GmbH).

Apoptosis analysis. Apoptotic cells were identified using an Annexin-V-FITC/PI apoptosis kit (cat. no. ads5001; Absin Bioscience Inc.) following the manufacturer's instructions. Briefly, CRC cells subjected to different treatments were collected, washed with PBS, and resuspended at a concentration of $1x10^6$ cells/ml. The cells were stained with 5 μl of Annexin V-FITC and 5 μl of PI in the dark at room temperature for 15 min. Samples were analyzed by flow cytometry (BD FACSCalibur; BD Biosciences) within 1 h, and data were processed using FlowJo v10 software (BD Biosciences). The apoptotic rate was calculated as the percentage of early apoptotic cells (Annexin V-FITC-positive/PI-negative) plus late apoptotic cells (Annexin V-FITC-positive/PI-positive).

Immunofluorescence staining. CRC cells from different groups were seeded onto sterile glass coverslips placed in 24-well plates at a density of $5x10^4$ cells per well and allowed to adhere overnight at 37˚C in a humidified incubator with 5% CO_2. After the indicated treatments, cells were washed three times with PBS at room temperature and fixed with 95% ethanol for 10 min at room temperature. The cells were then permeabilized with 0.4% Triton X-100 for 10 min at room temperature, followed by three washes with PBS. Subsequently, cells were blocked with 2% bovine serum albumin (BSA; Sigma-Aldrich) in PBS for 1 h at 37˚C and incubated with anti-LC3 primary antibody (1:200, cat. no. ab232940; Abcam) overnight at 4˚C. After washing with PBS (5 min x3, room temperature), cells were incubated with a fluorescein-conjugated secondary antibody (1:500 in 1% BSA; Alexa Fluor® 488-conjugated goat anti-rabbit IgG; Thermo Fisher Scientific, Inc.; cat. no. A-11008) for 1 h at 37˚C in the dark. The nuclei were then counterstained with DAPI (1 μg/ml) for 8-10 min at room temperature in the dark. After three additional washes with PBS, coverslips were mounted onto glass slides using antifade mounting medium and observed under a fluorescence microscope (Olympus Corporation).

In vivo tumorigenicity experiments. Male BALB/c nude mice (aged 4-5 weeks and weighing 16-20 g) were purchased from the Henan Skabes Biotechnology Co., Ltd. A total of 18 mice were used. The mice were housed under specific pathogen-free conditions in an air-filtered facility at 22±2˚C with a relative humidity of 50-60% and a 12 h light/12 h dark cycle, with unrestricted access to standard chow and water. A total of $5x10^6$ SW620 cells pre-transduced with Ad-sh-PLD2 or Ad-sh-NC were resuspended in 200 μl of PBS and subcutaneously injected into the right flank of nude mice to establish a CRC xenograft model. When the average tumor volume reached ~50 mm^3, mice were randomly assigned to three groups (n=6 per group): Ad-sh-NC, Ad-sh-PLD2 and Ad-sh-PLD2 + Rapa. 5-Fu was administered intraperitoneally at a dose of 50 mg/kg once daily for 7 consecutive days. Rapamycin (Rapa) was administered intraperitoneally at a dose of 2 mg/kg every other day throughout the treatment period. Tumor size was measured every 7 days using a digital caliper, and tumor volume was calculated

using the formula (length x width^2)/2. After 42 days, the mice were sacrificed by CO_2 inhalation using a gradual-fill method (30-70% chamber volume per minute) until loss of consciousness, followed by cervical dislocation to ensure death in accordance with the guidelines of the American Veterinary Medical Association (AVMA) for the euthanasia of animals (29). Tumors were collected, weighed, images captured and the tumors subjected to further analyses. All animal experiments were conducted with the approval of the Research Ethics Committee and according to the institutional guidelines of the Animal Care and Use Committee at the Shanxi Province Cancer Hospital (Shanxi, China; approval no. SM-21CA; 2022-4-12).

Immunohistochemistry analysis. The resected tumor tissues were immersed in formalin, dehydrated, embedded in paraffin and sectioned at a thickness of 4 μm. These sections were deparaffinized and rehydrated before being subjected to microwave treatment for antigen retrieval. After H_2O_2 was used to eliminate endogenous peroxidase activity and block nonspecific binding with 5% BSA (Beyotime Biotechnology) for 1 h at room temperature. Subsequently, the sections were incubated overnight at 4˚C with rabbit anti-Ki-67 primary antibody (cat. no. ab15580; 1:200; Abcam). After washing with PBS, the sections were incubated with HRP-conjugated goat anti-rabbit IgG secondary antibody (cat. no. A0208; 1:250; Beyotime Biotechnology) for 1 h at 37˚C. Immunoreactive signals were visualized using a 3,3'-diaminobenzidine (DAB) chromogenic detection kit (Beyotime Biotechnology) at room temperature for 3 min. The sections were counterstained with hematoxylin (Beyotime Biotechnology) at room temperature for 3 min, followed by rinsing in running water for 10 min. Finally, the stained sections were examined using a bright-field light microscope (Olympus Corporation) at x200 magnification and images of five randomly selected fields per sample were captured for analysis.

Western blotting. Total protein was extracted from tissues and cells using RIPA lysis buffer and quantified using a BCA protein kit (Beyotime Biotechnology). Equal quantities (30 μg) of protein samples were separated via 10-12% sodium dodecyl sulfate-polyacrylamide gel electrophoresis and transferred onto PVDF membranes (MilliporeSigma). The membranes were blocked with 5% non-fat milk in PBS for 1 h at room temperature and subsequently incubated overnight at 4˚C with primary antibodies against PLD2 (1:500; cat. no. ab192804), HIF-1α (1:1,000; cat. no. ab308637), MRP2 (1:1,000; cat. no. ab203397), Beclin-1 (1:1,000; cat. no. ab62557), caspase-3 (1:1,000; cat. no. ab44976), cleaved caspase-3 (1:500; cat. no. ab2302), LC3 (1:3,000; cat. no. ab51520), Ki-67 (1:1,000; cat. no. ab254123) and GAPDH (1:20,000; cat. no. ab128915) all obtained from Abcam (Fig. S1). After washing, the membranes were incubated with HRP-conjugated goat anti-rabbit IgG secondary antibody (cat. no. A0208; Beyotime Biotechnology) diluted 1:5,000 for 2 h at room temperature. Protein bands were visualized using an enhanced chemiluminescence detection kit (cat. no. RPN2232; Amersham; Cytiva). The grayscale values of all bands were analyzed using the ImageJ software (version 1.53e; National Institutes of Health).

Statistical analysis. For all statistical analyses, GraphPad Prism v. 8.0 (Dotmatics) was used. The results are presented as the mean ± standard deviation (SD). The differences between any two groups were determined by conducting Student's t-tests. To determine differences among multiple groups, one-way analysis of variance (ANOVA) was conducted, followed by Dunnett's or Tukey's post hoc test. $P<0.05$ was considered to indicate a statistically significant difference.

Results

Increased PLD2 expression is associated with poor prognosis and chemoresistance in CRC. Analysis conducted using the UALCAN database revealed that PLD2 mRNA expression was markedly higher in tumor tissues (n=286) than in normal tissues (n=41) from patients with colon adenocarcinoma (COAD; Fig. 1A). Furthermore, PLD2 expression exhibited variable differences across clinicopathological features, including cancer stage (Fig. 1B), histological subtype (Fig. 1C), and nodal metastasis status (Fig. 1D). The data from the Kaplan-Meier plotter database indicated that high expression of PLD2 was associated with a reduction in OS (Fig. 1E, P=0.00062, HR=1.44) and RFS (Fig. 1F; P=0.0029, HR=1.47) in CRC patients. Additionally, we comprehensively examined the PLD2 level in 20 cases of 5-Fu-sensitive tissues and 5-Fu-resistant tissues. The results demonstrated that the expression levels of PLD2 mRNA (Fig. 1G) and protein (Fig. 1H) were both considerably upregulated in 5-Fu-resistant tissues compared with 5-Fu-sensitive tissues. The protein expression of HIF-1α, MRP2, and Beclin-1 was greater in 5-Fu-resistant tissues than in 5-Fu-sensitive tissues (Fig. 1H).

Hypoxia triggers the expression of PLD2, HIF-1α, drug resistance and autophagy markers in CRC cells. To investigate the effects of hypoxia on PLD2 expression and autophagy in CRC cells, western blotting was performed to examine the expression levels of PLD2, HIF-1α, MRP2, Beclin-1 and the LC3-II/I ratio under hypoxic conditions. In SW620 cells (Fig. 2A), the protein levels of PLD2 and MRP2 increased gradually from 0 to 24 h of hypoxia but showed a slight decrease at 48 h, whereas the expression levels of HIF-1α and Beclin-1, as well as the LC3-II/I ratio, continued to increase progressively following exposure to hypoxia for 0, 12, 24 and 48 h. Quantitative analysis confirmed significant upregulation of these proteins, indicating that hypoxia activates both PLD2 expression and autophagy. In SW480 cells (Fig. 2B), similar trends were observed, with gradual increases in PLD2, HIF-1α, MRP2, and Beclin-1 expression and the LC3-II/I ratio over time. As 24 h of hypoxia induced marked changes in these protein markers, this time point was selected for subsequent experiments. These results, together with clinical tissue analysis showing higher PLD2 and MRP2 levels in 5-Fu-resistant CRC tissues, suggested that hypoxia-induced PLD2 upregulation may contribute to chemoresistance in CRC.

PLD2 reduces the chemosensitivity of CRC cells to 5-Fu under hypoxic conditions. To investigate the role of PLD2 in hypoxia-induced 5-Fu resistance, SW620 and SW480 cells were treated with varying concentrations of 5-Fu under

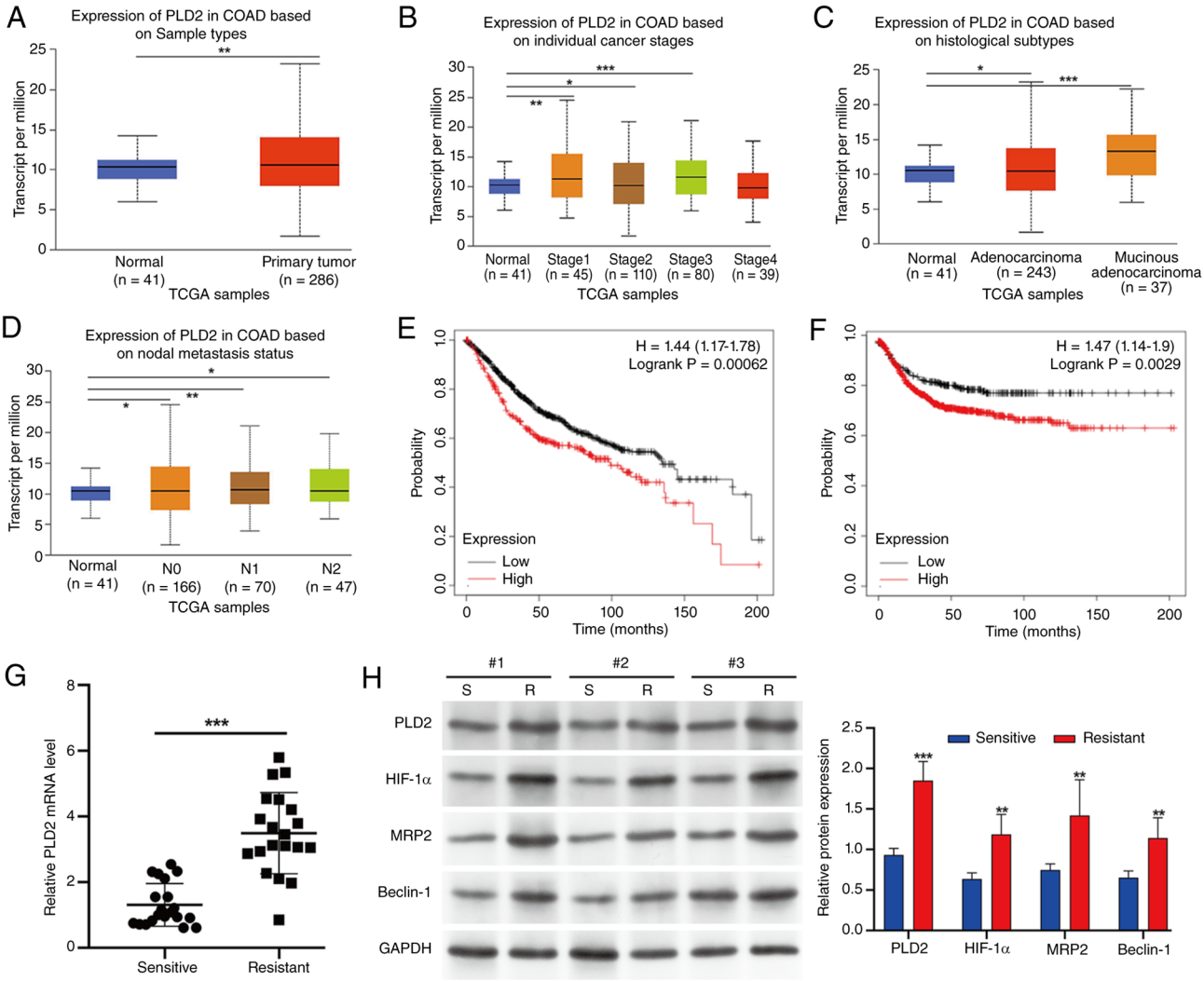

Figure 1. Elevated PLD2 expression correlates with poor prognosis and 5-Fu resistance in CRC. The PLD2 mRNA levels in COAD vs. adjacent tissues stratified by (A) sample type, (B) stage, (C) subtype and (D) metastasis status (UALCAN database). One-way analysis of variance followed by Dunnett's post hoc test was performed to compare among multiple groups. *P<0.05, **P<0.01, ***P<0.001 vs. Normal. Kaplan-Meier analysis of (E) overall and (F) recurrence-free survival by PLD2 expression. (G) PLD2 mRNA in 5-Fu-sensitive (n=20) vs. 5-Fu-resistant (n=20) tissues. (H) Representative PLD2, HIF-1α, MRP2 and Beclin-1 protein images (n=3 per group). Each value represents the mean ± SD from three biological/technical replicates. The comparison between sensitive and resistant groups was carried out using Student's t-test. **P<0.01, ***P<0.001 vs. sensitive group. PLD2, phospholipase D2; 5-Fu, 5-fluorouracil; CRC, colorectal cancer; COAD, colon adenocarcinoma; UALCAN, The University of Alabama at Birmingham cancer data analysis portal; HIF-1α, hypoxia-inducible factor 1 alpha; MRP2, multidrug resistance-associated protein 2; TCGA, The Cancer Genome Atlas; HR, hazard ratio.

normoxic and hypoxic conditions for 24 h. CCK-8 assays showed that 5-Fu reduced cell viability in a dose-dependent manner under both conditions, but cell survival under hypoxia was markedly higher than under normoxia (Fig. 3A), indicating that hypoxia attenuates 5-Fu cytotoxicity. Flow cytometry further confirmed that apoptosis induced by 5-Fu was lower under hypoxia compared with normoxia for both 4 and 8 μM concentrations (Fig. 3B). These findings indicate that hypoxia reduces 5-Fu sensitivity in CRC cells, rather than reflecting intrinsic or acquired differences in baseline drug resistance between SW620 and SW480 cells. For subsequent mechanistic experiments involving PLD2 overexpression or knockdown, SW620 cells were selected as a representative model, as 24 h hypoxia induced relatively higher PLD2 expression in SW620 cells than in SW480 cells (Fig. 3C). Importantly, the use of parental (non-resistant) CRC cell lines allowed systematic manipulation of PLD2 expression under controlled hypoxic conditions to directly assess its causal role in the acquisition of chemoresistance. PLD2 overexpression increased cell viability and reduced apoptosis following 5-Fu treatment, whereas PLD2 knockdown decreased viability and enhanced apoptosis in a dose-dependent manner (Fig. 3D and E). PLD2 overexpression decreased the cleaved caspase-3/total caspase-3 ratio and increased MRP2 and Beclin-1 expression, whereas PLD2 knockdown exerted the opposite effects. Notably, total caspase-3 expression remained relatively unchanged among groups (Fig. 3F). These results indicated that under hypoxia, PLD2 decreased 5-Fu sensitivity by inhibiting apoptosis and enhancing drug resistance and autophagy, linking hypoxic stress, PLD2 activation and chemoresistance.

PLD2 decreases the chemosensitivity of SW620 cells under hypoxia by promoting autophagy. To investigate how PLD2 reduces the response of CRC cells to 5-Fu under hypoxia,

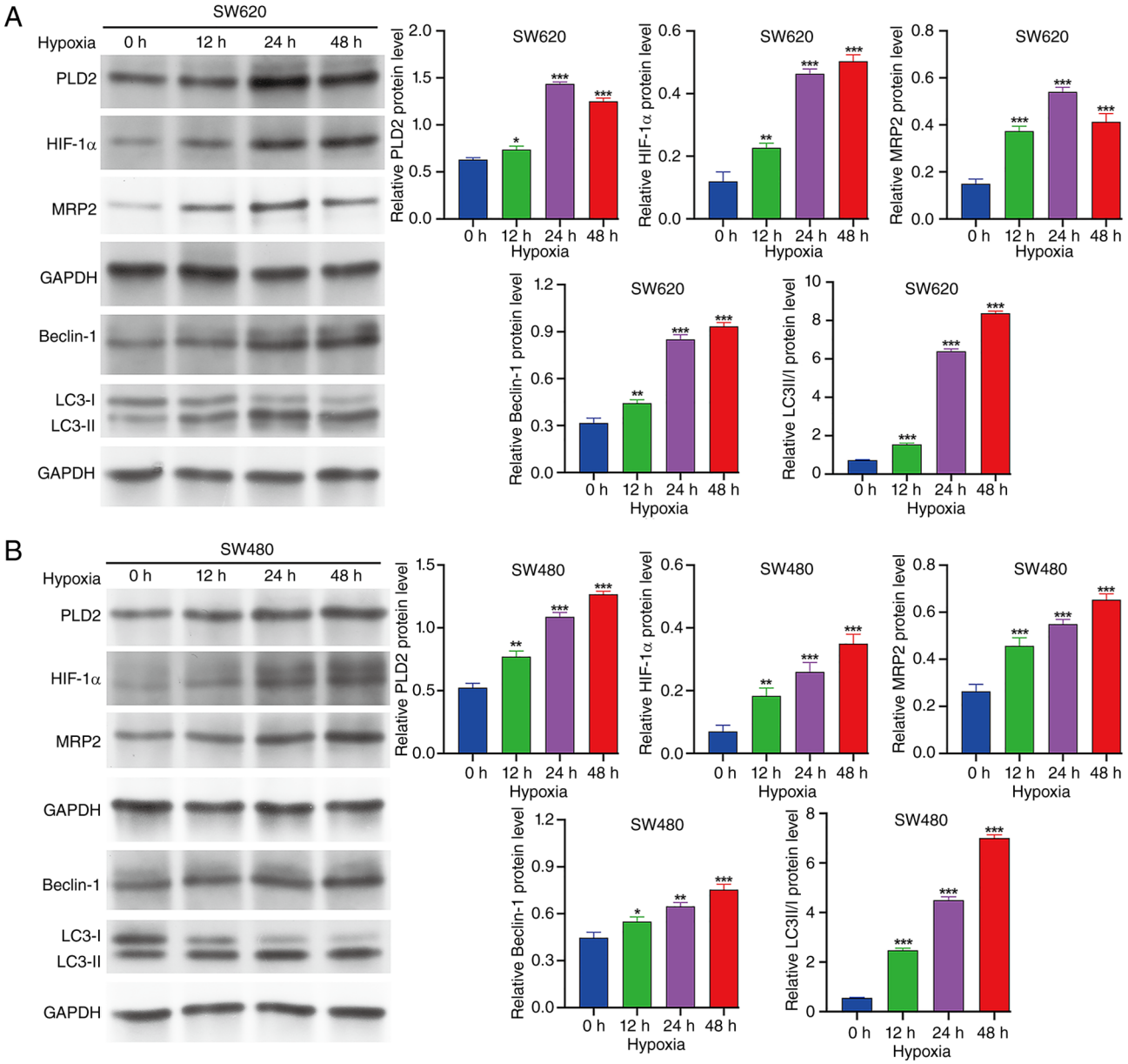

Figure 2. Hypoxia triggers the expression of PLD2, HIF-1α drug-resistance and autophagy markers in CRC cells. SW620 and SW480 cells exposed to hypoxia (0-48 h). (A and B) Western blotting of PLD2, HIF-1α, MRP2, Beclin-1, LC3-II/I with densitometry. Each value represents the mean ± SD from biological/technical replicates. *P<0.05, **P<0.01, ***P<0.001 vs. 0 h via one-way analysis of variance followed by Dunnett's post hoc test. PLD2, phospholipase D2; HIF-1α, hypoxia-inducible factor 1 alpha; CRC, colorectal cancer; MRP2, multidrug resistance-associated protein 2.

Rapa (10 μM, an autophagy activator) or 3-MA (10 mM, an autophagy inhibitor) was applied to SW620 cells. CCK-8 assays showed that autophagy activation partially reversed the reduced viability caused by PLD2 knockdown (Fig. 4A), while autophagy inhibition markedly counteracted the increased viability induced by PLD2 overexpression under 5-Fu treatment (Fig. 4B). Colony formation assays revealed that under hypoxia + 6 μmol/l 5-Fu, the reduced colonies in the Ad-sh-PLD2 group were restored by Rapa, whereas the elevated colonies in the Ad-oe-PLD2 group were markedly diminished by 3-MA (Fig. 4C). Flow cytometry confirmed that Rapa reversed the increase in apoptosis caused by PLD2 knockdown, while 3-MA rescued the decrease in apoptosis induced by PLD2 overexpression (Fig. 4D). Immunofluorescence staining showed that LC3 downregulation in the Ad-sh-PLD2 group was restored by Rapa, whereas the LC3 upregulation in the Ad-oe-PLD2 group was attenuated by 3-MA (Fig. 5A). Western blotting further demonstrated that PLD2 expression was partially restored by Rapa after knockdown and was more strongly reduced by 3-MA in PLD2-overexpressing cells. Correspondingly, the changes in cleaved caspase-3/total caspase-3 ratio, MRP2, and Beclin-1 levels were reversed by Rapa or 3-MA in the same patterns (Fig. 5B). These findings confirmed that PLD2 promoted autophagy-dependent 5-Fu resistance in SW620 cells under hypoxia.

PLD2 knockdown represses 5-Fu resistance via autophagy in vivo. To elucidate the role of PLD2 in the chemosensitivity of CRC cells *in vivo*, a xenograft tumor model was established in nude mice. SW620 cells pre-transduced with

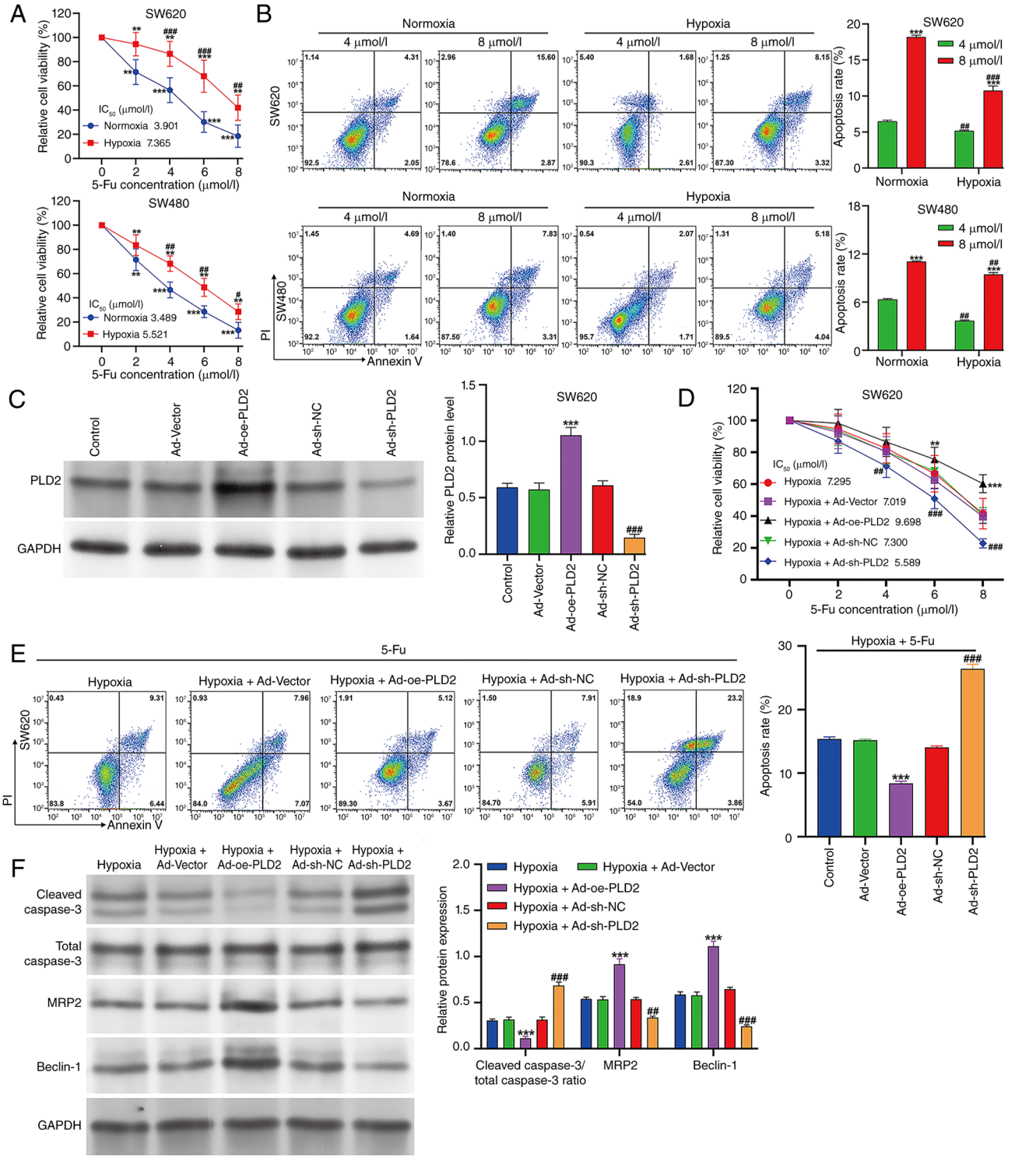

Figure 3. PLD2 reduces chemosensitivity of CRC cells to 5-Fu under hypoxia conditions. SW620 and SW480 cells treated with 5-Fu (0-8 μmol/l) under normoxia or hypoxia. (A) Cell viability was detected by CCK-8 assay (**P<0.01, ***P<0.001 vs. 0 μmol/l; $^{\#}$P<0.05, $^{\#\#}$P<0.01, $^{\#\#\#}$P<0.001 vs. normoxia) via Student's t-test; (B) Cell apoptosis was detected by flow cytometry assay with Annexin-V FITC/PI double staining. (***P<0.001 vs. 4 μmol/l; $^{\#\#}$P<0.01, $^{\#\#\#}$P<0.001 vs. normoxia) via Student's t-test. (C) PLD2 overexpression/knockdown efficiency by western blotting (***P<0.001 vs. Ad-Vector; $^{\#\#\#}$P<0.001 vs. Ad-sh-NC) via Student's t-test. (D) Viability and (E) apoptosis of SW620 cells transduced with Ad-sh-PLD2, Ad-oe-PLD2, or their corresponding control vectors under hypoxia + 5-Fu (**P<0.01, ***P<0.001 vs. Hypoxia + Ad-Vector; $^{\#\#}$P<0.01, $^{\#\#\#}$P<0.001 vs. Hypoxia + Ad-sh-NC) via Student's t-test. (F) Total caspase-3, cleaved caspase-3, MRP2 and Beclin-1 in SW620 treated with 6 μmol/l 5-Fu (***P<0.001 vs. Hypoxia + Ad-Vector; $^{\#\#}$P<0.01, $^{\#\#\#}$P<0.001 vs. Hypoxia + Ad-sh-NC). Each value represents the mean ± SD from three biological/technical replicates. PLD2, phospholipase D2; CRC, colorectal cancer; 5-Fu, 5-fluorouracil; Ad, adenoviral vector; sh, short hairpin; NC, negative control; oe, overexpression; MRP2, multidrug resistance-associated protein 2.

Ad-sh-PLD2 or Ad-sh-NC were subcutaneously inoculated. One week after cell injection, 5-Fu/Rapa was administered to the mice. As shown in Fig. 6A, tumors derived from Ad-sh-PLD2-transduced SW620 cells grew markedly more slowly than those from the Ad-sh-NC group and this inhibitory effect was partially reversed by Rapa treatment. By day 42,

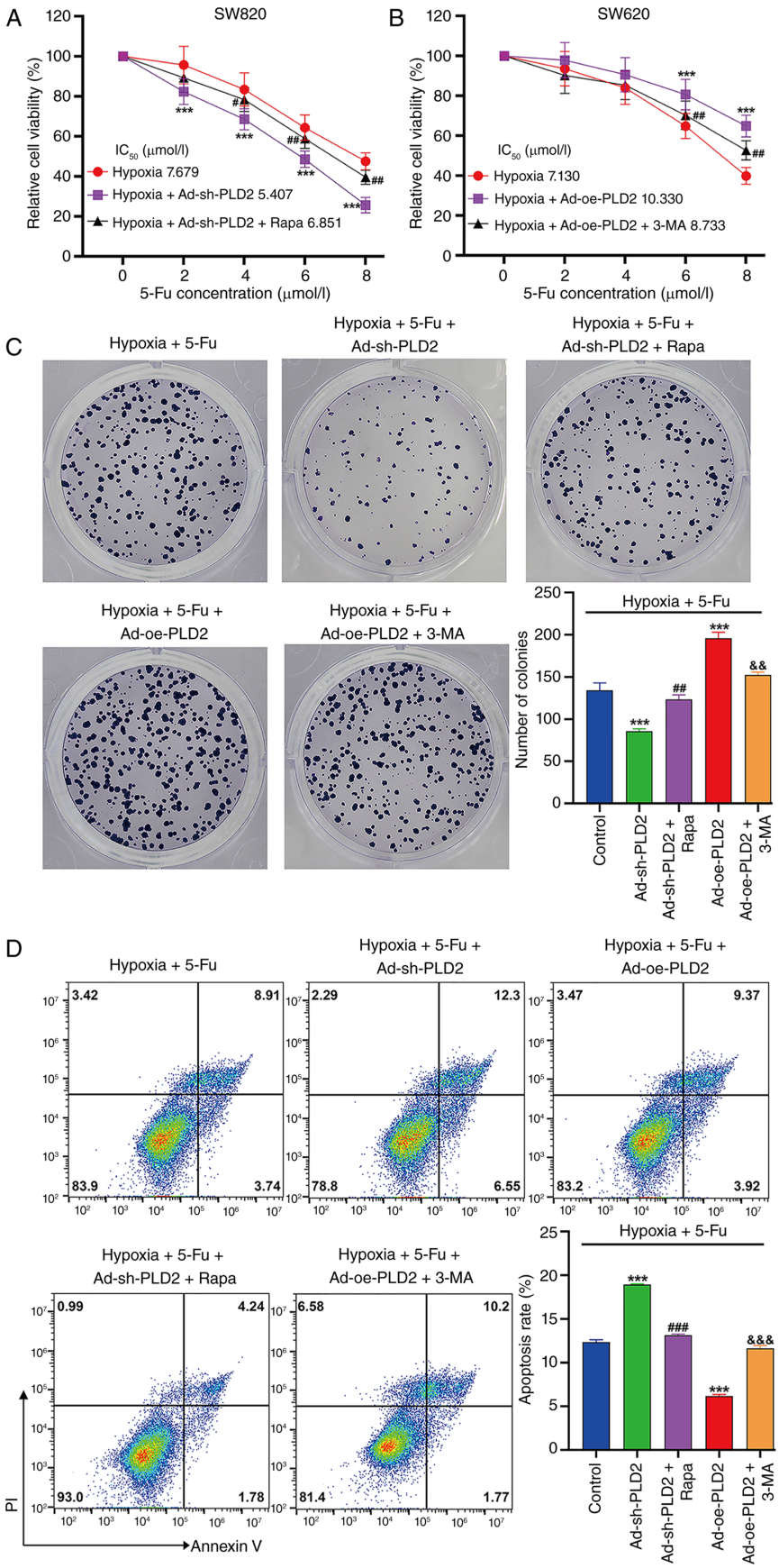

Figure 4. Autophagy modulation alters PLD2 effects on viability and apoptosis in hypoxic SW620 cells. (A and B) CCK-8 viability in Ad-sh-PLD2 + Rapa or Ad-oe-PLD2 + 3-MA cells treated with 5-Fu (0-8 μmol/l, 24 h) in SW620 cells (***P<0.001 vs. hypoxia; $^{\#}$P<0.05, $^{\#\#}$P<0.01 vs. hypoxia + Ad-sh-PLD2 or hypoxia + Ad-oe-PLD2) via one-way analysis of variance followed by Tukey's post hoc test; (C) Colony formation and (D) Annexin-V/PI apoptosis assays at 6 μmol/l 5-Fu (***P<0.001 vs. control; $^{\#\#}$P<0.01, $^{\#\#\#}$P<0.001 vs. Ad-sh-PLD2; $^{\&\&}$P<0.01, $^{\&\&\&}$P<0.001 vs. Ad-oe-PLD2) via one-way analysis of variance, followed by Tukey's post hoc test; Each value represents the mean ± SD from three biological/technical replicates. PLD2, phospholipase D2; 5-Fu, 5-fluorouracil; Ad, adenoviral vector; sh, short hairpin; NC, negative control; oe, overexpression; Rapa, rapamycin.

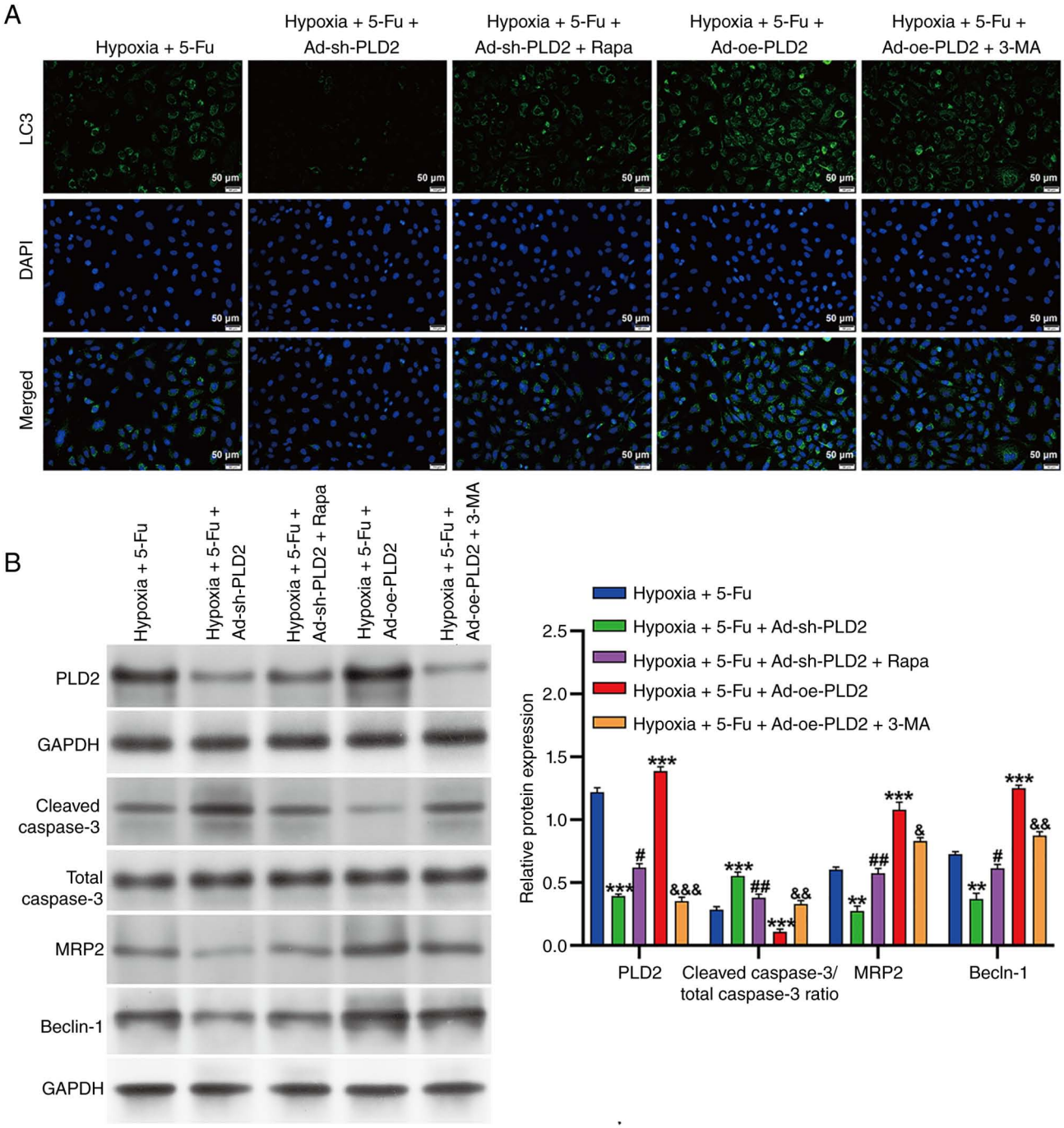

Figure 5. Autophagy modulation alters PLD2 effects on apoptosis and autophagy markers. SW620 cells (Ad-sh-PLD2 ± Rapa or Ad-oe-PLD2 ± 3-MA) treated with 6 μmol/l 5-Fu under hypoxia. (A) Representative immunofluorescence staining images of LC3. Scale bar, 50 μm. (B) The protein levels of PLD2, total caspase-3, cleaved caspase-3, MRP2, and Beclin-1 were analyzed (**P<0.01, ***P<0.001 vs. hypoxia + 5-Fu; $^{\#}$P<0.05, $^{\#\#}$P<0.01 vs. hypoxia + 5-Fu + Ad-sh-PLD2; $^{\&}$P<0.05, $^{\&\&}$P<0.01, $^{\&\&\&}$P<0.001 vs. hypoxia + 5-Fu + Ad-oe-PLD2) via one-way analysis of variance followed by Tukey's post hoc test. Each value represents the mean ± SD from three biological/technical replicates. PLD2, phospholipase D2; Ad, adenoviral vector; sh, short hairpin; NC, negative control; oe, overexpression; 5-Fu, 5-fluorouracil; MRP2, multidrug resistance-associated protein 2; Rapa, rapamycin.

both tumor volume (Fig. 6B) and tumor weight (Fig. 6C) were markedly reduced in the Ad-sh-PLD2 group under 5-Fu treatment compared with controls, whereas Rapa treatment attenuated this reduction. Additionally, reduced protein levels of Ki-67 were confirmed in xenograft tumor tissues from the Ad-sh-PLD2 group (Fig. 6D), and this effect was alleviated by Rapa treatment. Consistently, Western blotting showed that PLD2, Ki-67 and MRP2 expression levels, as well as the LC3-II/LC3-I ratio, were reduced in tumors derived from Ad-sh-PLD2-transduced cells, and these effects were reversed by Rapa treatment (Fig. 6E). These findings suggested that PLD2 knockdown suppresses 5-Fu resistance of CRC *in vivo*, potentially through inhibition of autophagy.

Discussion

Chemotherapeutic agents such as 5-Fu are the primary treatment options for solid tumors, including CRC. However, the

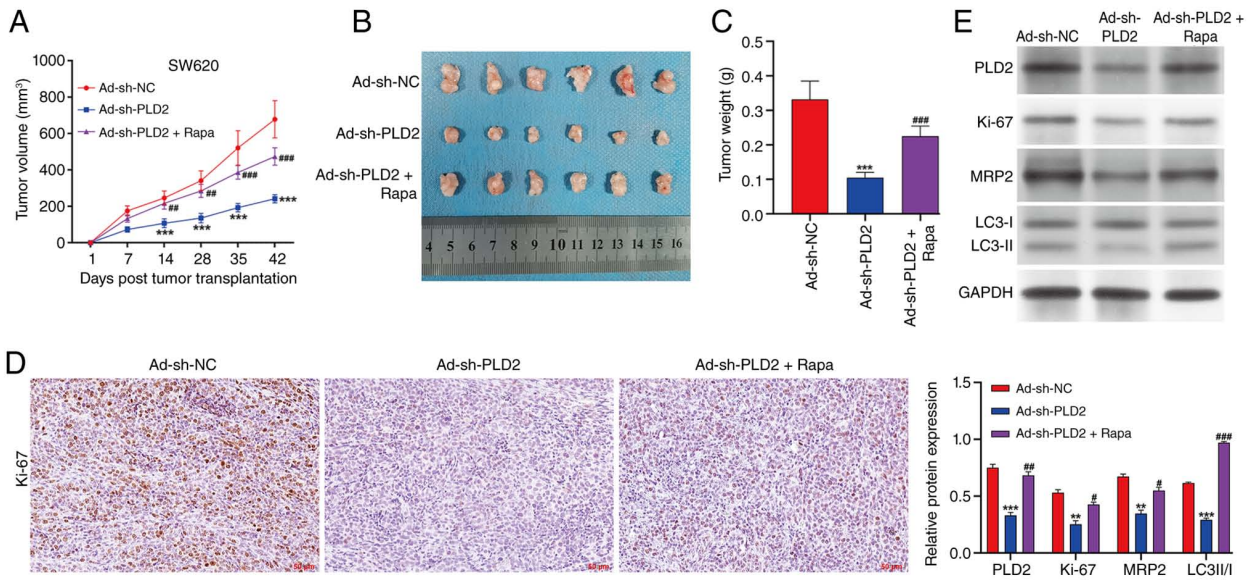

Figure 6. PLD2 knockdown suppresses 5-Fu resistance via autophagy *in vivo*. BALB/c nude mice (n=6 per group) inoculated with SW620 cells (Ad-sh-PLD2 or Ad-sh-NC). When tumors reached ~50 mm³, mice received 5-Fu (50 mg/kgx7 days) ± Rapa. (A) Tumor volume was continuously monitored for 42 days. On day 42, the xenografts were (B) removed and (C) weighed. (D) The protein expression of Ki-67 in xenograft tumor tissues was determined by immunohistochemistry assay (magnification, x200; scale bar, 50 μm). (E) The protein levels of PLD2, Ki-67, MRP2, and LC3-II/I in xenograft tumor tissues were measured (**P<0.01, ***P<0.001 vs. Ad-sh-NC; $^{\#}$P<0.05, $^{\#\#}$P<0.01, $^{\#\#\#}$P<0.001 vs. Ad-sh-PLD2) via one-way analysis of variance followed by Tukey's post hoc test. Each value represents the mean ± SD from three biological/technical replicates. PLD2, phospholipase D2; 5-Fu, 5-fluorouracil; Ad, adenoviral vector; sh, short hairpin; NC, negative control; oe, overexpression; Rapa, rapamycin.

emergence of drug resistance poses a substantial impediment to cancer therapy. Hypoxia, a state defined by oxygen deficiency, can trigger various changes in tumor cells, including the dysregulation of genes and signaling pathways associated with cell survival and the conferral of drug resistance (30). The role of hypoxia-induced autophagy in chemoresistance has become quite prominent (31,32). Consequently, elucidating the mechanisms involved in the development of chemoresistance and identifying biomarkers specific to hypoxia-induced autophagy are highly important for formulating effective therapeutic strategies.

Several studies have suggested that PLD2 acts as an oncogene and is involved in multiple facets of tumorigenesis, such as the induction of angiogenin in renal cell carcinoma (33) and prevention of apoptosis in breast cancer (34) and squamous cell carcinoma (35). In another study, we verified that PLD2 is upregulated in CRC and positively regulates tumor growth (19). The present study conducted bioinformatics analysis and found that increased PLD2 expression is associated with poor prognosis in CRC patients, which is supported by the findings of Saito *et al* (18), who reported a significant correlation between the PLD expression level and the survival of CRC patients. By collecting specimens, the present study found that PLD2 expression was considerably higher in 5-Fu-resistant tissues compared with that in 5-Fu-sensitive tissues. Moreover, HIF-1α, MRP2 and Beclin-1 were markedly increased in 5-Fu-resistant samples. Hypoxia-induced stress leads to chemoresistance by activating hypoxia-inducible factor 1α (HIF-1α) and inducing protective autophagy, thereby disrupting cancer therapy in the tumor microenvironment (36). Consistent with the data from the tissue samples, hypoxia triggered the expression of PLD2, HIF-1α, MRP2 and Beclin-1 and the LC3-II/I ratio in SW620 and SW480 cells in a

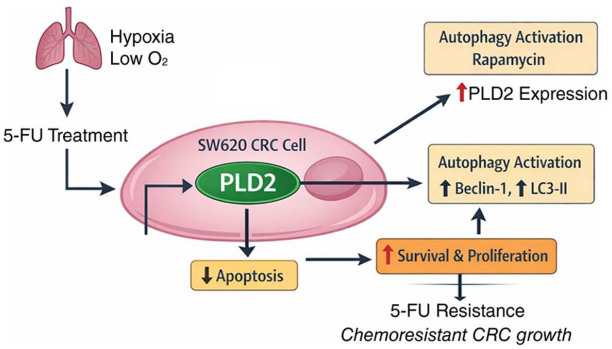

Figure 7. Schematic model of PLD2-mediated hypoxia-induced 5-Fu resistance in CRC cells. PLD2, phospholipase D2; 5-Fu, 5-fluorouracil; CRC, colorectal cancer.

time-dependent manner. These results strongly indicated that PLD2 may be largely responsible for the chemoresistance of CRC cells under hypoxia, which is consistent with the findings observed in ovarian tumors (22).

The present study subsequently investigated the mechanisms through which PLD2 augments chemoresistance in CRC cells under hypoxia. Initially, it was found that hypoxia-induced PLD2 expression counteracted the apoptotic signal triggered by 5-Fu, thereby contributing to drug resistance. When PLD2 inhibition was combined with 5-Fu treatment under hypoxic conditions, the apoptotic marker cleaved caspase-3 increased, whereas the levels of MRP2 and Beclin-1 decreased. CRC cells under hypoxia are more resistant to chemotherapy than cells under normoxia (37), indicating that hypoxia in the tumor microenvironment is a major contributor to chemoresistance (38). The present study further showed that knocking down PLD2 reduced cell viability and increased apoptosis

in SW620 cells. As revealed by CCK-8 and apoptosis assays, activation of autophagy partially reversed the effects of PLD2 knockdown on the response of SW620 cells to 5-Fu under hypoxia. Similarly, PLD2 inhibition markedly upregulated cleaved caspase-3 and downregulated MRP2 and Beclin-1 expression, indicating that PLD2 decreases chemosensitivity by promoting autophagy. Notably, the data also indicated that autophagy activation, for example by Rapa, can lead to increased PLD2 expression. This may reflect a compensatory cellular response, as PLD2 interacts with autophagy-related pathways and participates in adaptive stress responses, potentially forming a positive feedback loop that further enhances cell survival and 5-Fu resistance. Autophagy plays a protective role in cancer by providing nutrients, oxygen and invasive channels for tumors (39). Hypoxia-induced autophagy can be mediated via activating transcription factor 4 (ATF4) (40), HIF-1α (41) and AMP-activated protein kinase (42). Our previous study revealed that PLD2 expression in SW620 cells is upregulated via HIF-1α in response to hypoxic stress, highlighting that HIF-1α-induced PLD2 plays a key role in tumor growth (19). These findings suggest that PLD2 is a central mediator of hypoxia-induced autophagy and chemoresistance and that autophagy itself may further amplify PLD2 expression, forming a feedback loop that sustains survival and drug resistance.

From a translational perspective, PLD2 represents a promising therapeutic target. Several small-molecule PLD inhibitors (such as FIPI and VU0155069) have shown preclinical efficacy, but their specificity, pharmacokinetics, and potential toxicity are major hindrances to clinical development (43,44). Moreover, although targeting autophagy is conceptually attractive, clinical translation is difficult because autophagy can play dual roles in tumors, either by promoting survival or increasing cell death, depending on the context. Early clinical trials using autophagy inhibitors such as hydroxychloroquine have shown modest results, with limited efficacy and challenges in achieving sufficient concentrations for sustained autophagy inhibition (45-47). These findings highlight the need for combination strategies and predictive biomarkers to identify responsive patients. Therefore, PLD2 inhibition in hypoxic CRC may be effective but requires careful evaluation in preclinical models and clinical studies to optimize safety, efficacy, and patient selection.

In summary, the present study indicated that HIF-1α-induced PLD2 plays a central role in hypoxia-induced autophagy and chemoresistance in CRC. Hypoxia upregulated the expression of PLD2, HIF-1α, MRP2 and Beclin-1 in both 5-Fu-resistant tissues and CRC cells. Functional assays showed that PLD2 overexpression reduced 5-Fu-induced apoptosis under hypoxic conditions, whereas PLD2 silencing restored chemosensitivity, underscoring its critical role in mediating hypoxia-driven drug resistance. Furthermore, bidirectional modulation of autophagy using rapamycin or 3-MA revealed that autophagy can, in turn, influence PLD2 expression, suggesting a potential positive feedback loop in SW620 cells acquiring resistance (Fig. 7). These results highlighted PLD2 as a promising therapeutic target in hypoxic CRC, although further validation in larger patient cohorts is warranted.

The present study had several limitations. First, autophagy was evaluated mainly by static markers (LC3-II/I, Beclin-1) and pharmacological modulators (Rapa, 3-MA), which cannot fully distinguish between increased autophagy and impaired degradation. Future studies should validate these findings using direct flux assays, such as tandem mCherry-GFP-LC3 reporters or lysosomal inhibitors. Second, although the data strongly supported the hypothesis that PLD2 enhances autophagy to promote 5-Fu resistance, the specific downstream signaling pathway involved remains to be elucidated. Third, more selective genetic approaches (such as ATG5/ATG7 knockdown) may help confirm that autophagy is required for PLD2-mediated chemoresistance. Fourth, while it was observed that hypoxia-induced HIF-1α upregulated PLD2 expression, it remains unclear whether this regulation is direct (via promoter binding) or indirect and further experiments are needed to clarify the underlying mechanism. Fifth, while the current *in vivo* experiments used PLD2 knockout models, future studies could explore the therapeutic potential of targeting PLD2 with selective inhibitors in CRC, which would provide additional validation for its role in chemoresistance. These issues need to be addressed in future studies to increase the mechanistic understanding of PLD2-driven autophagy in hypoxia-induced drug resistance.

Acknowledgements

Not applicable.

Funding

The present study received funding from Natural Science Foundation of Shanxi Province (grant no. 202303021211226), The Science and Education Cultivation Fund of the National Cancer and Regional Medical Center of Shanxi Provincial Cancer Hospital (grant no. QH2023002) and Key Research and Development Program of Shaanxi Province (grant no. 2024SF-ZDCYL-02-11).

Availability of data and materials

The data generated in the present study may be requested from the corresponding author.

Authors' contributions

JYZ, WDW and MXL conceived and designed the study, supervised the experiments, and wrote the manuscript. KLD, PFW and XSY performed the experiments, collected and analyzed the data. YJL and YW contributed to data analysis, interpretation and manuscript review. JYZ and WDW confirm the authenticity of all the raw data. All authors read and approved the final manuscript.

Ethics approval and consent to participate

The present study was approved by the Ethics Committee of the Shanxi Province Cancer Hospital (Shanxi, China; approval no. SPCH-87A; Date: 2021-1-21) and was conducted in accordance with the principles of the Declaration of Helsinki. Written informed consent was obtained from all participants. All animal experiments were approved by the Animal Ethics

Committee of the Shanxi Province Cancer Hospital (Shanxi, China; approval no. SM-21CA; Date: 2022-4-12) and were conducted in compliance with institutional guidelines and the ARRIVE guidelines (https://arriveguidelines.org/).

Patient consent for publication

Not applicable.

Competing interests

The authors declare that they have no competing interests.

References

1. Siegel RL, Wagle NS, Cercek A, Smith RA and Jemal A: Colorectal cancer statistics, 2023. CA Cancer J Clin 73: 233-254, 2023.
2. Morris VK, Kennedy EB, Baxter NN, Benson AB III, Cercek A, Cho M, Ciombor KK, Cremolini C, Davis A, Deming DA, *et al*: Treatment of metastatic colorectal cancer: ASCO Guideline. J Clin Oncol 41: 678-700, 2023.
3. Vodenkova S, Buchler T, Cervena K, Veskrnova V, Vodicka P and Vymetalkova V: 5-fluorouracil and other fluoropyrimidines in colorectal cancer: Past, present and future. Pharmacol Ther 206: 107447, 2020.
4. Li Y, Wang Z, Ajani JA and Song S: Drug resistance and Cancer stem cells. Cell Commun Signal 19: 19, 2021.
5. Al Tameemi W, Dale TP, Al-Jumaily RMK and Forsyth NR: Hypoxia-modified cancer cell metabolism. Front Cell Dev Biol 7: 4, 2019.
6. Weng X, Ma T, Chen Q, Chen BW, Shan J, Chen W and Zhi X: Decreased expression of H19/miR-675 ameliorates hypoxia-induced oxaliplatin resistance in colorectal cancer. Heliyon 10: e27027, 2024.
7. Li X, Zhou Y, Li Y, Yang L, Ma Y, Peng X, Yang S, Liu J and Li H: Autophagy: A novel mechanism of chemoresistance in cancers. Biomed Pharmacother 119: 109415, 2019.
8. Kovale L, Singh MK, Kim J and Ha J: Role of Autophagy and AMPK in cancer stem cells: Therapeutic opportunities and obstacles in cancer. Int J Mol Sci 25: 8647, 2024.
9. Li Q, Ni Y, Zhang L, Jiang R, Xu J, Yang H, Hu Y, Qiu J, Pu L, Tang J and Wang X: HIF-1alpha-induced expression of m6A reader YTHDF1 drives hypoxia-induced autophagy and malignancy of hepatocellular carcinoma by promoting ATG2A and ATG14 translation. Signal Transduct Target Ther 6: 76, 2021.
10. Yang X, Yin H, Zhang Y, Li X, Tong H, Zeng Y, Wang Q and He W: Hypoxia-induced autophagy promotes gemcitabine resistance in human bladder cancer cells through hypoxia-inducible factor 1α activation. Int J Oncol 53: 215-224, 2018.
11. Notte A, Ninane N, Arnould T and Michiels C: Hypoxia counteracts taxol-induced apoptosis in MDA-MB-231 breast cancer cells: Role of autophagy and JNK activation. Cell Death Dis 4: e638, 2013.
12. Qi Y, Qi W, Liu S, Sun L, Ding A, Yu G, Li H, Wang Y, Qiu W and Lv J: TSPAN9 suppresses the chemosensitivity of gastric cancer to 5-fluorouracil by promoting autophagy. Cancer Cell Int 20: 4, 2020.
13. Zheng Y, Wu J, Chen H, Lin D, Chen H, Zheng J, Xia H, Huang L and Zeng C: KLF4 targets RAB26 and decreases 5-FU resistance through inhibiting autophagy in colon cancer. Cancer Biol Ther 24: 2226353, 2023.
14. Ghim J, Chelakkot C, Bae YS, Suh PG and Ryu SH: Accumulating insights into the role of phospholipase D2 in human diseases. Adv Biol Regul 61: 42-46, 2016.
15. Wang Z, Zhang F, He J, Wu P, Tay LWR, Cai M, Nian W, Weng Y, Qin L, Chang JT, *et al*: Binding of PLD2-Generated phosphatidic acid to KIF5B promotes MT1-MMP surface trafficking and lung metastasis of mouse breast cancer cells. Dev Cell 43: 186-197. e7, 2017.
16. Noble AR, Hogg K, Suman R, Berney DM, Bourgoin S, Maitland NJ and Rumsby MG: Phospholipase D2 in prostate cancer: Protein expression changes with Gleason score. Br J Cancer 121: 1016-1026, 2019.
17. Oshimoto H, Okamura S, Yoshida M and Mori M: Increased activity and expression of phospholipase D2 in human colorectal cancer. Oncol Res 14: 31-37, 2003.
18. Saito M, Iwadate M, Higashimoto M, Ono K, Takebayashi Y and Takenoshita S: Expression of phospholipase D2 in human colorectal carcinoma. Oncol Rep 18: 1329-1334, 2007.
19. Liu M, Du K, Fu Z, Zhang S and Wu X: Hypoxia-inducible factor 1-alpha up-regulates the expression of phospholipase D2 in colon cancer cells under hypoxic conditions. Med Oncol 32: 394, 2015.
20. Liu M, Fu Z, Wu X, Du K, Zhang S and Zeng L: Inhibition of phospholipaseD2 increases hypoxia-induced human colon cancer cell apoptosis through inactivating of the PI3K/AKT signaling pathway. Tumour Biol 37: 6155-6168, 2016.
21. Liu M, Du K, Jiang B and Wu X: High expression of PhospholipaseD2 induced by hypoxia promotes proliferation of colon cancer cells through activating NF-κ Bp65 signaling pathway. Pathol Oncol Res 26: 281-290, 2020.
22. Munoz-Galvan S, Verdugo-Sivianes EM, Santos-Pereira JM, Estevez-Garcia P and Carnero A: Essential role of PLD2 in hypoxia-induced stemness and therapy resistance in ovarian tumors. J Exp Clin Cancer Res 43: 57, 2024.
23. Hwang WC, Kim MK, Song JH, Choi KY and Min do S: Inhibition of phospholipase D2 induces autophagy in colorectal cancer cells. Exp Mol Med 46: e124, 2014.
24. Chandrashekar DS, Bashel B, Balasubramanya SAH, Creighton CJ, Ponce-Rodriguez I, Chakravarthi B and Varambally S: UALCAN: A portal for facilitating tumor subgroup gene expression and survival analyses. Neoplasia 19: 649-658, 2017.
25. Lánczky A and Győrffy B: Web-based survival analysis tool tailored for medical research (KMplot): Development and implementation. J Med Internet Res 23: e27633, 2021.
26. Livak KJ and Schmittgen TD: Analysis of relative gene expression data using real-time quantitative PCR and the 2(-Delta Delta C(T)) method. Methods 25: 402-408, 2001.
27. Wang W, Li X, Cui C, Yin G, Ren W and Wang X: Autophagy of umbilical cord mesenchymal stem cells induced by rapamycin conduces to pro-angiogenic function of the conditioned medium. Biochem Biophys Rep 36: 101583, 2023.
28. Chicote J, Yuste VJ, Boix J and Ribas J: Cell death triggered by the autophagy inhibitory drug 3-Methyladenine in growing conditions proceeds with DNA damage. Front Pharmacol 11: 580343, 2020.
29. Leary S, Underwood W, Anthony R, Cartner S, Grandin T, Greenacre C, Gwaltney-Brant S, McCrackin MA, Meyer R, Miller D, *et al*: AVMA guidelines for the euthanasia of animals: 2020 edition. American Veterinary Medical Association, Schaumburg, IL, 2020.
30. Weng X, Liu H, Ruan J, Du M, Wang L, Mao J, Cai Y, Lu X, Chen W, Huang Y, *et al*: HOTAIR/miR-1277-5p/ZEB1 axis mediates hypoxia-induced oxaliplatin resistance via regulating epithelial-mesenchymal transition in colorectal cancer. Cell Death Discov 8: 310, 2022.
31. Vasilevskaya IA, Selvakumaran M, Roberts D and O'Dwyer PJ: JNK1 Inhibition Attenuates Hypoxia-induced autophagy and sensitizes to chemotherapy. Mol Cancer Res 14: 753-763, 2016.
32. Dong Y, Wu Y, Zhao GL, Ye ZY, Xing CG and Yang XD: Inhibition of autophagy by 3-MA promotes hypoxia-induced apoptosis in human colorectal cancer cells. Eur Rev Med Pharmacol Sci 23: 1047-1054, 2019.
33. Kandori S, Kojima T, Matsuoka T, Yoshino T, Sugiyama A, Nakamura E, Shimazui T, Funakoshi Y, Kanaho Y and Nishiyama H: Phospholipase D2 promotes disease progression of renal cell carcinoma through the induction of angiogenin. Cancer Sci 109: 1865-1875, 2018.
34. Hwang WC, Kang DW, Kang Y, Jang Y, Kim JA and Min DS: Inhibition of phospholipase D2 augments histone deacetylase inhibitor-induced cell death in breast cancer cells. Biol Res 53: 34, 2020.
35. Wang X, Tao C, Yuan C, Ren J, Yang M and Ying H: AQP3 small interfering RNA and PLD2 small interfering RNA inhibit the proliferation and promote the apoptosis of squamous cell carcinoma. Mol Med Rep 16: 1964-1972, 2017.
36. D'Orazi G and Cirone M: Mutant p53 and cellular stress pathways: A criminal alliance that promotes cancer progression. Cancers (Basel) 11: 614, 2019.
37. Zichittella C, Barreca MM, Cordaro A, Corrado C, Alessandro R and Conigliaro A: Mir-675-5p supports hypoxia-induced drug resistance in colorectal cancer cells. BMC Cancer 22: 567, 2022.

38. Cosse JP and Michiels C: Tumour hypoxia affects the responsiveness of cancer cells to chemotherapy and promotes cancer progression. Anticancer Agents Med Chem 8: 790-797, 2008.
39. Rakesh R, PriyaDharshini LC, Sakthivel KM and Rasmi RR: Role and regulation of autophagy in cancer. Biochim Biophys Acta Mol Basis Dis 1868: 166400, 2022.
40. Rzymski T, Milani M, Singleton DC and Harris AL: Role of ATF4 in regulation of autophagy and resistance to drugs and hypoxia. Cell Cycle 8: 3838-3847, 2009.
41. Liu XW, Su Y, Zhu H, Cao J, Ding WJ, Zhao YC, He QJ and Yang B: HIF-1alpha-dependent autophagy protects HeLa cells from fenretinide (4-HPR)-induced apoptosis in hypoxia. Pharmacol Res 62: 416-425, 2010.
42. Kim J, Kundu M, Viollet B and Guan KL: AMPK and mTOR regulate autophagy through direct phosphorylation of Ulk1. Nat Cell Biol 13: 132-141, 2011.
43. Hwang WC, Song D, Lee H, Oh C, Lim SH, Bae HJ, Kim ND, Han G and Min DS: Inhibition of phospholipase D1 induces immunogenic cell death and potentiates cancer immunotherapy in colorectal cancer. Exp Mol Med 54: 1563-1576, 2022.
44. Lee SK, Kim YS, Bae GH, Lee HY and Bae YS: VU0155069 inhibits inflammasome activation independent of phospholipase D1 activity. Sci Rep 9: 14349, 2019.
45. Amaravadi RK, Lippincott-Schwartz J, Yin XM, Weiss WA, Takebe N, Timmer W, DiPaola RS, Lotze MT and White E: Principles and current strategies for targeting autophagy for cancer treatment. Clin Cancer Res 17: 654-666, 2011.
46. Amaravadi RK, Kimmelman AC and Debnath J: Targeting autophagy in cancer: Recent advances and future directions. Cancer Discov 9: 1167-1181, 2019.
47. Onorati AV, Dyczynski M, Ojha R and Amaravadi RK: Targeting autophagy in cancer. Cancer 124: 3307-3318, 2018.

Copyright © 2026 Du et al. This work is licensed under a Creative Commons Attribution-NonCommercial-NoDerivatives 4.0 International (CC BY-NC-ND 4.0) License.